Design of the Square Loop Frequency Selective Surfaces with Particle Swarm Optimization via the Equivalent Circuit Model

Asim Egemen YILMAZ[1], *Mustafa KUZUOGLU*[2]

[1] Dept. of Electronics Engineering, Ankara University, Tandogan, 06100 Ankara, Turkey
[2] Dept. of Electrical and Electronics Engineering, Middle East Technical University, 06530, Ankara, Turkey

aeyilmaz@eng.ankara.edu.tr, kuzuoglu@metu.edu.tr

Abstract. *In this study, Particle Swarm Optimization is applied for the design of Square Loop Frequency Selective Surfaces (the conventional Square Loop, Gridded Square Loop, and Double Square Loop) via their equivalent circuits. For this purpose, first the derivation of the equivalent circuit formulation is revisited. Then an objective function, which is based on the transmission coefficients at various frequencies at the pass/stop-bands, is defined. By means of an ANSI C++ implementation, a platform independent console application (which depends on the Equivalent Circuit Models and continuous form of Particle Swarm Optimization) is developed. The obtained results are compared to those in the literature. It is observed that the Particle Swarm Optimization is perfectly suitable for this sort of problems, and the solution accuracy is limited to and dominated by that of the Equivalent Circuit Model.*

Keywords

Artificial electromagnetic material, equivalent circuit model, frequency selective surface, particle swarm optimization, periodic structure.

1. Introduction

A Frequency Selective Surface (FSS) can be considered to be a surface construction serving as a filter for plane waves at any angles of incidence. It has been widely used in broadband communications, radar systems, and antenna technology. Recently, it also triggers researchers for applications of periodic structures like electromagnetic band-gap structures and doubly negative materials etc. FSSs, which are typically constructed by means of doubly-periodic surface elements, have angular dependent behaviors as well as band pass/stop-band frequency dependent characteristics.

The development of novel design methodologies for the FSSs is also an attractive area for researchers. The parameters to be adjusted during the design can be the type, shape, size, loading, spacing and the orientation of the element. Since the relevant parameter selection is a process depending on the trial-error method; nature-inspired population based methods such as the Genetic Algorithm (GA), Differential Evolution Strategy (DES), and Particle Swarm Optimization (PSO) have been applied for this purpose recently (for example [1]-[8]).

The problems regarding the design of FSSs fall into two main categories:

- The problems in which the pattern of the periodic structure is to be determined;
- The problems in which the parameters of a fixed pattern are to be determined.

For the first class of problems, discrete domain algorithms (such as GA or discrete/binary PSO) are more suitable and easily applicable. On the other hand, for the second class, where the optimized design parameters (such as the geometrical dimensions inside to pattern such as width, length, etc.) are to be determined, continuous domain algorithms (such as DES and PSO) are more suitable. In this study, the element type is assumed to be various forms of Square Loop; and the approach is to adjust the parameters such as element size and spacing for desired features. For the optimization purpose, PSO is chosen.

In most of the papers published so far, the fitness/objective function is dependent to the result obtained by full wave analysis methods, such as the Periodic Method of Moments. In the nature-inspired population based methods, it is necessary to compute the fitness/objective function numerous times (in the order of tens of thousands). Coupling the population based optimization methods with the full wave analysis methods might yield a time consuming, sometimes even an unfeasible optimization process. In this study, instead of trying to analyze the behavior by the accurate but time consuming Periodic Method of Moments; the Equivalent Circuit Model, which works for square loop FSSs with acceptable accuracy in a rapid manner, is preferred.

2. Square Loop FSSs and the Equivalent Circuit Model

The Square Loop FSSs in the literature have several forms, three of which are seen in Fig. 1 together with their design parameters.

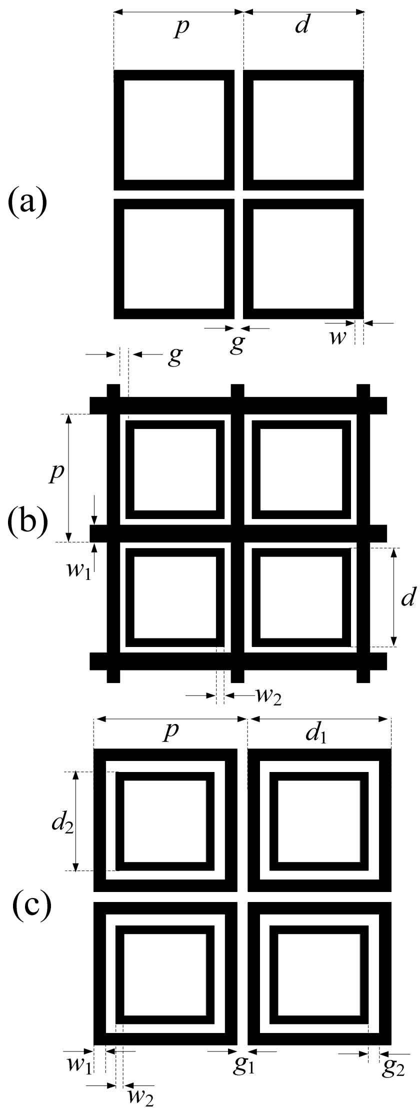

Fig. 1. Square loop FSSs and design parameters: (a) the conventional square loop (SL), (b) gridded square loop (GSL), and (c) double square loop (DSL).

When the plane-wave transmission responses are considered, it can be seen that transmission characteristics of the conventional Square Loop consist of a single reflection band and a lower-frequency transmission band. Typically, transmission/reflection band ratios higher than 2.5:1 can be obtained. For the Gridded Square Loop FSSs, the presence of a grid modifies the low-frequency transmission response by giving a more closely spaced frequency-band ratio between 1.3:1 and 2:1. For these structures, the band centers are relatively insensitive to the angle of incidence; but the bandwidths are sensitive. On the other hand, Double Square Loop is essentially a double-resonant structure, providing a stable low-frequency reflection band coupled with a closely spaced high-frequency transmission band. Wider frequency-band separations up to 2.2:1 can be achieved by means of the Double Square Loop FSSs. All these structures can be approximately represented with resonant circuits consisting of inductances and capacitances via the Equivalent Circuit Model.

The Equivalent Circuit Model is based on the theory proposed by Marcuvitz [9], who developed the initial expression for the periodic gratings. The technique was first applied to the frequency selective surfaces by Anderson [10]. It gives reasonable results compared to the measured ones; however, it can be directly applied to only a limited range of structures. Although it is possible to add a variety of circuit elements to the equivalent circuit for complicated structures, the validity of the model is not guaranteed. The technique is not easily applicable to multilayer FSS geometries since it does not support the effects of the dielectric substrate and superstrate; and also non-normal incidence has limited validity. Langley, Parker et al. found reasonable results for Square Loop FSSs, and even for Jerusalem Cross FSSs for normal incidence [11]-[14]. However, the accuracy of their model was unacceptable for oblique angles. Throughout in this study, we preferred to use the improved equivalent circuit model developed by Lee and Langley [15], which is more accurate and also valid for oblique incidence.

2.1 Derivation of the Equivalent Circuit Model

The idea behind the equivalent circuit model can be explained as follows: Consider a series of metallic strips residing on a plane; where the width of each strip is w, the distance between two successive strips is d, and the periodicity of the strips is p. Consider that a plane wave is incident on this series with angles (θ, ϕ), as seen in Fig. 2.

Transmission through such geometry can be modeled by using a duality with a transmission line of characteristic impedance equal to that of free space, on which a lumped reactance representing the strip array is mounted [9].

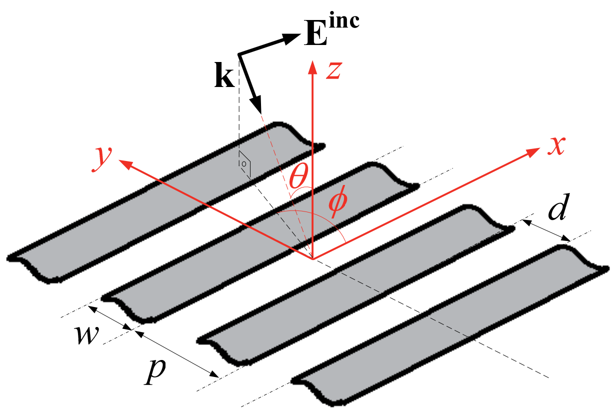

Fig. 2. A series of metallic strips residing on a surface; and a plane wave incident onto it.

If the tangential component of the incident electric field is parallel to the conductors, then this reactance is inductive, allowing very little transmission at low frequencies; and hence the inductance virtually short circuits the line. If the periodicity p decreases, or the width w increases; then the inductance decreases, and the grid behaves similar to a solid metallic surface, as expected. With such a quantitative deduction, it can be said that the value of the inductance depends on p and w, the angles of incidence (θ, ϕ), and whether the incidence is TE or TM.

For this case, the normalized immittance expressions of the strip grating were given by Marcuvitz as [9]:

$$X_{TE} = F(p,w,\lambda) = \frac{p\cos\theta}{\lambda}\left[\ln\csc\left(\frac{\pi w}{2p}\right) + G(p,w,\lambda,\theta)\right] \tag{1}$$

where λ is the wavelength. The susceptance for TM-incidence can be found from Babinet's duality conditions as:

$$B_{TM} = 4F(p,d,\lambda) = \frac{4p\cos\phi}{\lambda}\left[\ln\csc\left(\frac{\pi d}{2p}\right) + G(p,d,\lambda,\phi)\right] \tag{2}$$

Certainly, (1) and (2) are valid if $w \ll p$, $d \ll p$, and $p \ll \lambda$. Similarly, the TM-incidence inductance and the TE-incidence capacitance can be written as follows:

$$X_{TM} = \frac{p\sec\phi}{\lambda}\left[\ln\csc\left(\frac{\pi w}{2p}\right) + G(p,w,\lambda,\phi)\right] \tag{3}$$

$$B_{TE} = \frac{4p\sec\theta}{\lambda}\left[\ln\csc\left(\frac{\pi d}{2p}\right) + G(p,d,\lambda,\theta)\right] \tag{4}$$

In order to preserve the continuity of the text, the definition of the correction term G is skipped here, but given in the Appendix. The transmission coefficient τ can now be determined from the normalized admittance of the array at oblique incidence:

$$|\tau|^2 = \frac{4}{4+|Y|^2}. \tag{5}$$

2.2 Equivalent Circuits of Square Loop FSSs

According to the formulations given in the previous subsection, the equivalent circuits of the square loop frequency selective circuits were defined, and the values of the terms seen in Fig. 3 were derived in [15] and [16].

The admittance of the SL-FSS is calculated by using the equivalent circuit seen in Fig. 3(a) is given in [16] as:

$$Y = \frac{1}{B_1 + X_1} \tag{6}$$

where B_1 and X_1 are given as:

$$B_1 = \omega C_1 = 4.0\cdot F(p,g,\lambda)\cdot(d/\varepsilon_r p), \tag{7}$$

$$X_1 = \omega L_1 = F(p,2w,\lambda)\cdot(d/p). \tag{8}$$

On the other hand, the admittance of the GSL-FSS is calculated by using the equivalent circuit seen in Fig. 3(b):

$$Y = -j\left(\frac{1-\omega^2 C_1(L_1+L_2)}{\omega L_2(1-\omega^2 C_1 L_1)}\right) \tag{9}$$

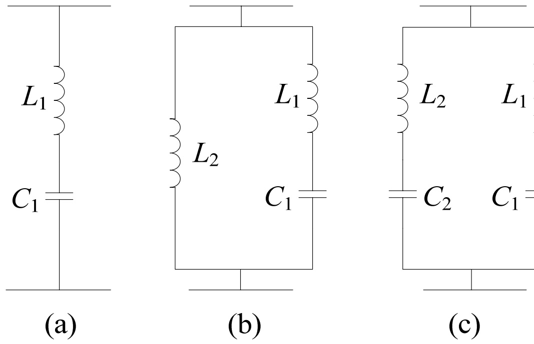

Fig. 3. Equivalent circuits of: (a) the conventional square loop (SL), (b) gridded square loop (GSL), and (c) double square loop (DSL).

Equivalently, Y can be written in a neater form as follows:

$$Y = j\left[\left(\frac{B_1}{1-X_1B_1}\right) - \frac{1}{X_2}\right] \tag{10}$$

where the terms in (10) are given in [15] as:

$$B_1 = \omega C_1 = 2.0\cdot\varepsilon_r\cdot F(p,g,\lambda)\cdot(d/p), \tag{11}$$

$$X_1 = \omega L_1 = 2(X_2 \parallel X_3), \tag{12}$$

$$X_2 = \omega L_2 = F(p,w_1,\lambda), \tag{13}$$

$$X_3 = F(p,2w_2,\lambda)\cdot(d/p), \tag{14}$$

and finally, the admittance of the DSL-FSS is calculated by using the equivalent circuit seen in Fig. 3(c):

$$Y = j\omega\left(\frac{C_1+C_2-\omega^2 C_1C_2(L_1+L_2)}{(1-\omega^2C_1L_1)(1-\omega^2C_2L_2)}\right) \tag{15}$$

Equivalently, Y can be written in a more compact form as follows:

$$Y = j\left[\left(\frac{B_1}{1-X_1B_1}\right) + \left(\frac{B_2}{1-X_2B_2}\right)\right] \tag{16}$$

where the terms in (16) are given in [15] as:

$$B_1 = \omega C_1 = 0.75\cdot B_{1p}\cdot(d_1/p), \tag{17}$$

$$B_2 = \omega C_2 = \frac{B_{1p}B_{2p}}{B_{1p}+B_{2p}}\cdot(d_2/p), \tag{18}$$

$$B_{1p} = 4.0\cdot\varepsilon_r\cdot F(p,g_1,\lambda), \tag{19}$$

$$B_{2p} = 4.0\cdot\varepsilon_r\cdot F(p,g_2,\lambda), \tag{20}$$

$$X_1 = \omega L_1 = 2.0 \cdot \frac{X_{1p} X_{2p}}{X_{1p} + X_{2p}} \cdot (d_1 / p), \quad (21)$$

$$X_2 = \omega L_2 = F(p, 2w_2, \lambda) \cdot (d_2 / p), \quad (22)$$

$$X_{1p} = F(p, w_1, \lambda), \quad (23)$$

$$X_{2p} = F(p, w_2, \lambda). \quad (24)$$

3. The Solution Procedure

For the solution of the design problem (i.e. determination of the design parameters illustrated in Fig. 1), first an objective function depending on the transmission coefficients, which are computed at various frequencies inside the band of concern, is defined. For each type of square loop, the design problem is described as a multi-dimensional continuous optimization problem, where the number of dimensions is determined by the number of design parameters to be adjusted. Instead of using a totally-chance oriented trial-error method, the multi-dimensional search operation is performed in systematically by means of swarm intelligence (the Particle Swarm Optimization, particularly). In the following subsections, mathematical foundations of the implementation are given.

3.1 The Objective Function

There are three factors describing the performance of an FSS:

- the width of the pass-band or the stop band,
- the roll-off rate (the –0.5 / –10.0dB band edge ratio),
- the stability of the transmission response to angle of wave incidence.

Hence, by taking N_{pass} test frequencies in the passband, and N_{stop} frequencies in the stopband

$$f(\mathbf{x}) = W_{-0.5dB} \left\{ \sum_{i=1}^{N_{pass}} \left| \tau_i + 0.5 \right| \right\} + W_{-10.0dB} \left\{ \sum_{j=1}^{N_{stop}} \left| \tau_j + 10 \right| \right\} \quad (25)$$

where τ_i is the transmission coefficient (as in (5)) calculated for a fixed frequency, and the weighting coefficients are defined as:

$$W_{-0.5dB} = \begin{cases} 0 & \text{if } \tau_i \geq -0.5\text{dB in the passband} \\ 1 & \text{otherwise} \end{cases} \quad (26)$$

$$W_{-10.0dB} = \begin{cases} 0 & \text{if } \tau_i \leq -10.0\text{dB in the stopband} \\ 1 & \text{otherwise} \end{cases} \quad (27)$$

3.2 Particle Swarm Optimization

Particle Swarm Optimization is a method proposed by Eberhart and Kennedy [17] after getting influenced by the behaviors of the animals living as colonies/swarms. Similar to the members of the swarms individually searching for the best place for nutrition in 3-dimensional space, the method depends on motions of particles (swarm members) searching for the global best in N-dimensional continuous space. The position of each particle is a solution candidate, and every time the fitness of this solution is recomputed. In addition to its exploration capability (i.e. the tendency for random search throughout the domain), each particle has a cognitive behavior (i.e. remembering its own good memories and having tendency to return there); as well as a social behavior (i.e. observing the rest of the swarm and having tendency to go where most other particles go). The parametric representation of all these tendencies and the balance among them are the keys for the success and the power of the method.

So far, the method has been successfully applied to various multidimensional continuous and discontinuous problems; and especially after its introduction to the electromagnetics society by Robinson and Rahmat-Samii [18], various researches have been applying the method to various inverse problems in electromagnetics. A recent review article by Poli [19] demonstrates how wide the application spectrum of the method currently is.

All particles are initialized at random positions inside the search space with random velocities. For an n-dimensional optimization problem, let us assume that the position and the velocity vectors of a particle at the ith iteration are denoted by $\mathbf{x}^{(i)} = [x_1^{(i)}\ x_2^{(i)}\ \ldots\ x_n^{(i)}]$ and $\mathbf{v}^{(i)} = [v_1^{(i)}\ v_2^{(i)}\ \ldots\ v_n^{(i)}]$, respectively. At the ith iteration of the algorithm, the position and velocity components of each particle at the kth dimension are updated as follows:

$$v_k^{(i+1)} = w v_k^{(i)} + c_1 u_1 (pbest - x_k^{(i)}) + c_2 u_2 (gbest - x_k^{(i)}), \quad (28)$$

$$x_k^{(i+1)} = x_k^{(i)} + v_k^{(i+1)} \Delta t \quad (29)$$

where these two operations are repeated for all dimensions. The iterations are repeated until the exit criterion is met. In these equations; the so-called inertial weight w, is a measure indicating the tendency to preserve the velocity along the previous course. The term inertial weight was not included in the original PSO paper; it was introduced later by Shi and Eberhart [20] in order to improve the performance of the method. Moreover, in a following study they showed that the ideal choice for the inertial weight is to decrease it linearly from 0.95 to 0.4 [21]. c_1 and c_2 are measures indicating the tendencies of approaching to *pbest* and *gbest*, which are the personal and global best positions, respectively. For recent PSO works, 1.494 seems to be the most preferred value for c_1 and c_2. u_1 and u_2 are random numbers between 0.0 and 1.0; and the time step size Δt is usually taken to be unity for simplicity. The exit criteria for the termination of iterations might be of various forms such as a predefined total iteration number, total number of fitness computations, saturation in improvement in *gbest*, etc.

At each dimension, some restrictions can be defined applied on the movement of the particles, which are referred to as boundary conditions [18]. By means of these rules, which are revisited and re-defined by Xu and Rahmat-Samii [22], in a controlled manner, all the particles are inhibited to go out of the search space.

4. Results

In order to verify the applicability of the proposed method to the Square Loop FSS design problems, some examples are solved and the solutions are compared to the ones existing in the literature.

For all problems, at all dimensions, the search domain is limited due to the following factors:

- The upper limit for the periodicity is determined by the beginning of grating lobes $\lambda < p(1+\sin\theta)$, where λ is the wavelength, and θ is the maximum angle of incidence.
- On the other hand, the technological constraints impose additional limitations to the optimization parameters. In other words, the dimensions of the frequency selective surfaces have practical lower limits due to the manufacturing technology.

Reflecting boundary conditions (according to the definition given in [22]) are implemented in order to keep the particles inside the search domain.

Moreover, the following parameters are chosen for all the problems to be defined in the following subsections:

- The swarm size is taken to be 50.
- The number of iterations is chosen as 500 (i.e. objective function evaluated 25000 times for a single PSO execution).
- In order to evaluate the overall success of the method, 100 independent PSO executions are performed, and the averages of results obtained from all executions are computed. In other words, the value of each design parameter, which will be presented throughout Tab. 1 to Tab. 3, is the average value of the results obtained from 100 independent executions.

4.1 Example regarding the Conventional Square Loop FSS

The first example deals with the design of the conventional Square Loop FSSs, where 6 different problems given by Parker in [16] are solved. In this set of problems, the frequency band between 2 and 30 GHz is traced with a step size of 0.1 GHz (i.e. a total of 280 test frequencies). For this geometry, since $p = d + g$ by definition (see Fig. 1), the problem is reduced to a 3-dimensional one. The ranges for the remaining optimization parameters are defined: 4.0 mm $\leq p \leq$ 10.0 mm, 0.10 mm $\leq w \leq$ 2.0 mm, and 3.0 mm $\leq d \leq$ 7.0 mm. The obtained dimensions (in millimeters) are shown and compared to those of [16] in Tab. 1.

Problem	Results	*p*	*w*	*d*
1	[16]	5.25	0.47	5.0
	This Study	5.250	0.464	4.999
2	[16]	4.15	0.30	3.95
	This Study	4.149	0.301	3.951
3	[16]	4.31	0.31	3.95
	This Study	4.309	0.310	3.946
4	[16]	4.35	0.18	4.06
	This Study	4.344	0.178	4.046
5	[16]	4.80	0.23	4.41
	This Study	4.799	0.224	4.402
6	[16]	4.35	0.30	4.07
	This Study	4.344	0.299	4.061

Tab. 1. Obtained dimensions (mm) for the conventional square loop FSS problem (Parker [16] vs. this study).

4.2 Examples regarding the Gridded Square Loop FSS

This time, the examples given by Lee and Langley in [15] for the GSL-FSSs are solved. For these problems, the frequency band between 10 and 40 GHz is traced with a step size of 0.1 GHz (i.e. a total of 300 test frequencies). It should be noted that, for this geometry, since $p = d+w_1+2g$ by definition (see Fig. 1), the problem is reduced to a 4-dimensional one. The search range of the optimization parameters is set as follows: 3.0 mm $\leq p \leq$ 10.00 mm, 0.1 mm $\leq w_1 \leq$ 2.0 mm, 0.1 mm $\leq w_2 \leq$ 2.0 mm, and 2.5 mm $\leq d \leq$ 8.0 mm. The obtained dimensions (in millimeters) are shown and compared to those of [15] in Tab. 2.

Problem	Results	*p*	w_1	*d*	w_2
1	[15]	4.5	0.33	3.47	0.17
	This Study	4.440	0.317	3.461	0.178
2	[15]	5.05	0.15	3.7	0.15
	This Study	5.030	0.151	3.707	0.149
3	[15]	5.02	0.15	4.09	0.15
	This Study	5.008	0.144	4.110	0.154
4	[15]	5.02	0.09	4.19	0.2
	This Study	5.019	0.090	4.188	0.188
5	[15]	5.48	0.27	4.41	0.7
	This Study	5.466	0.264	4.423	0.709
6	[15]	6.0	0.2	4.6	0.8
	This Study	6.008	0.209	4.599	0.799

Tab. 2. Obtained dimensions (mm) for the gridded square loop FSS problem (Lee and Langley [15] vs. this study).

4.3 Example regarding the Double Square Loop FSS

Finally, the example given by Luo et al. in [3] and [6] for the DSL-FSSs is solved. For this problem, the frequency band between 2 and 18 GHz is traced with a step size of 0.1 GHz (i.e. a total of 160 test frequencies). In this problem, the maximum frequency of interest is about 18 GHz; and hence, the upper limit of p is 9.76 mm, which is the value for angle incidence of 45°. It should be noted that, for this geometry, since $p = d_1 + g_1$ by definition (see Fig. 1), the problem is reduced to a 5-dimensional one.

As in [3] and [6], the search range of the optimization parameters is set as follows: 3.0 mm ≤ p ≤ 9.76 mm, 0.2 mm ≤ w_1 ≤ 2.0 mm, 0.2 mm ≤ w_2 ≤ 2.0 mm, 0.2 mm ≤ g_1 ≤ 2.0 mm, and 0.2 mm ≤ g_2 ≤ 2.0 mm. The obtained dimensions (in millimeters) for normal incidence are shown and compared to those of [3] and [6] in Tab. 3.

Results	p	w_1	w_2	g_1	g_2
[3] & [6]	8.08	0.93	0.238	0.548	0.369
This Study	8.081	0.929	0.240	0.551	0.373

Tab. 3. Obtained dimensions (mm) for the DSL-FSS problem (Luo et al. [3]&[6] vs. this study).

5. Discussions and Conclusion

PSO is a powerful tool for the solution of complex multidimensional optimization problems both in continuous and discrete domains. The results of this study, which coincide with those in the literature, demonstrate that the method is also applicable for the design of various forms of Square Loop FSSs.

The software, which is a platform independent console application developed with ANSI C++ during this research, provides rapid solutions (over multiple independent solutions) in order of seconds at an ordinary laptop or desktop PC. The main issue in this study (and certainly for other similar studies) is the validity and the accuracy of the Equivalent Circuit Model. In the corresponding references (i.e. [3], [6], [15], and [16]), the discrepancies between the computed (by using the Equivalent Circuit Model) and measured transmission responses have already been given. The responses slightly differ due to the approximations in the Equivalent Circuit Model. On the other hand, it should be noted that, the correction factor $G()$ has considerable impact on the performance of the model, as it has been demonstrated in [15]. Hence, the current model used in our study with the correction factor seems to be of acceptable accuracy even for the oblique incidence.

As stated before, the Equivalent Circuit Model also suffers from several factors such as ease of generalization, modeling complex geometries with superstrates, etc. But in conclusion, whenever an accurate model is available and full wave analysis software packages are unavailable, the technique provides a practical means for rapid design parameter determination and selection. Two proposals can be made at this point:

1. Performing the global search with the equivalent circuit model rapidly and continuing the fine-tuning with a more accurate full wave analysis method; or
2. Trying to obtain more generic and more accurate equivalent circuit models (such as those of Dubrovka et al. [23]) and to use them.

For the currently ongoing work regarding this research study, the second option is chosen and being followed. The results obtained for other FSS geometries will be shared with the academic society in the near future.

Acknowledgements

The first author would like to express his gratitude to Dr. C. K. Lee for providing the 1985 dated proceeding (i.e. [15]) which includes the formulations of the correction factor $G()$. The authors would also like to express their gratitude to the anonymous reviewers for their careful inspections and fruitful comments for the improvement of the paper.

References

[1] MANARA, G., MONORCHIO, A., MITTRA, R. Frequency selective surface design based on genetic algorithm. *Electronics Letters*, 1999, vol. 35, no 17, p. 1400 – 1401.

[2] KERN, D. J., WERNER, D. H., WILHELM, M. J., CHURCH, K. H. Genetically engineered multiband high-impedance frequency selective surfaces. *Microwave and Optical Technology Letters*, 2003, vol. 38, no. 5, p. 400 – 403.

[3] LUO, X. F., LEE, C. K., QING, A. Design of frequency-selective surfaces (FSS) using differential evolution strategy (DES). In *Proceedings of the 27th ESA Antenna Technologies Workshop*. Santiago de Compostela (Spain), 2004, p. 201 – 207.

[4] LUO, X. F., QING, A., LEE, C. K. Application of the differential-evolution strategy to the design of frequency-selective surfaces. *International Journal of RF and Microwave Computer-Aided Engineering*, 2005, vol. 15, no. 2, p. 173 – 180.

[5] BOSSARD, J. A., WERNER, D. H., MAYER, T. S., DRUPP, R. P. A novel design methodology for reconfigurable frequency selective surfaces using genetic algorithms. *IEEE Transactions on Antennas and Propagation*, 2005, vol. 53, no. 4, p. 1390 – 1400.

[6] LUO, X. F., TEO, P. T., QING, A., LEE, C. K. Design of double-square-loop frequency-selective surfaces using differential evolution strategy coupled with equivalent-circuit model. *Microwave and Optical Technology Letters*, 2005, vol. 44, p. 159 – 162.

[7] GENOVESI, S., MITTRA, R., MONORCHIO, A., MANARA, G. Particle swarm optimization for the design of frequency selective surfaces. *IEEE Antennas and Wireless Propagation Letters*, 2006, vol. 5, p. 277 – 279.

[8] WU, G., HANSEN, V., KREYSA, E., GEMÜND H. -P. Optimization of FSS band-pass filters by means of swarm

intelligence (particle swarm optimization). *Advances in Radio Science*, 2006, vol. 4, p. 65 – 71 (in German).

[9] MARCUWITZ, N. *Waveguide Handbook*. 1st ed. New York: McGraw-Hill, 1951.

[10] ANDERSON, I. On the theory of self-resonant grids. *Bell System Technical Journal*, 1975, vol. 54, p. 1725 – 1731.

[11] HAMDY, S. M. A., PARKER, E. A. Comparison of modal analysis and equivalent circuit representation of E-plane of the Jerusalem cross. *Electronics Letters*, 1982, vol. 18, no. 2, p. 94 –95.

[12] LANGLEY, R. J., DRINKWATER, A. J. An improved empirical model for the Jerusalem cross. *IEE Proceedings H - Microwaves Optics and Antennas*, 1982, vol. 129, no. 1, p. 1 – 6.

[13] LANGLEY, R. J., PARKER, E. A. Equivalent circuit model for arrays of square loops. *Electronics Letters*, 1982, vol. 18, no. 7, p. 294 – 296.

[14] LANGLEY, R. J., PARKER, E. A. Double square frequency selective surfaces and their equivalent circuit. *Electronics Letters*, 1983, vol. 19, no. 17, p. 675 – 677.

[15] LEE, C. K., LANGLEY, R. J. Equivalent-circuit models for frequency selective surfaces at oblique angles of incidence. *IEE Proceedings H - Microwaves Optics and Antennas*, 1985, vol. 132, p. 395 – 399.

[16] PARKER, E. A. The gentleman's guide to frequency selective surfaces. Presented in *17th Q.M.W. Antenna Symposium,* London (UK), 1991.

[17] KENNEDY J., EBERHART, R. C. Particle swarm optimization. In *Proceedings of the IEEE Conference on Neural Networks*, Perth (Australia), 1995, p. 1942 – 1948.

[18] ROBINSON, J., RAHMAT-SAMII, Y. Particle swarm optimization in electromagnetics. *IEEE Transactions on Antennas and Propagation*, 2004, vol. 52, no. 2, p. 397 – 407.

[19] POLI, R. Analysis of the publications on the applications of particle swarm optimisation. *Journal of Artificial Evolution and Applications*, 2008, Article ID: 685175, doi:10.1155/2008/685175.

[20] SHI, Y., EBERHART, R. C. A modified particle swarm optimizer. In *Proc. of the IEEE International Conference on Evolutionary Computation*. Anchorage - AK (USA), 1998, p. 69 – 73.

[21] SHI, Y., EBERHART, R. C. Empirical study of particle swarm optimization. In *Proceedings of the Congress of Evolutionary Computing*. Piscataway - NJ (USA), 1999, p. 1945 – 1950.

[22] XU, S., RAHMAT-SAMII, Y. Boundary conditions in particle swarm optimization revisited. *IEEE Transactions on Antennas and Propagation*, 2007, vol. 55, no. 3, p. 760 – 765.

[23] DUBROVKA, R., VAZQUEZ, J., PARINI, C., MOORE, D. Equivalent circuit method for analysis and synthesis of frequency selective surfaces, *IEE Proceedings: Microwaves, Antennas and Propagation*, 2006, vol. 153, no. 3, p. 213 – 220.

[24] ARCHER, M. J. Wave reactance of thin planar strip gratings. *International Journal of Electronics*, 1985, vol. 58, p. 187 – 230.

About Authors ...

Asim Egemen YILMAZ was born in 1975. He received his B.Sc. degrees in Electrical-Electronics Engineering and Mathematics from the Middle East Technical University in 1997. He received his M.Sc. and Ph.D. degrees in Electrical-Electronics Engineering from the same university in 2000 and 2007, respectively. He is currently with the Dept. of Electronics Engineering in Ankara University, where he is an Assistant Professor. His research interests include computational electromagnetics, nature-inspired optimization algorithms, knowledge-based systems; more generally software development processes and methodologies.

Mustafa KUZUOGLU was born in 1957. He received his B.Sc., M.Sc., and Ph.D. degrees in Electrical-Electronics Engineering from the Middle East Technical University in 1979, 1981, and 1986, respectively; where he is currently a Professor. His research interests include computational electromagnetic, inverse problems, and radar.

Appendix

In [24], Archer derived the general expressions of the normalized wave reactances of inductive strip gratings. The first-order correction term *G*() is obtained from these expressions as:

$$G(p,d,\lambda,\tfrac{\theta}{\phi}) = \frac{A}{B} \tag{A.1}$$

where

$$A = 0.5(1-\beta^2)^2\left[\left(1-\frac{\beta^2}{4}\right)(C_{+1}+C_{-1}) + 4\beta^2 C_{+1}C_{-1}\right], \tag{A.2}$$

$$B = \left(1-\frac{\beta^2}{4}\right) + \beta^2\left(1+\frac{\beta^2}{2}-\frac{\beta^4}{8}\right)\cdot(C_{+1}+C_{-1}) + 2\beta^6 C_{+1}C_{-1} \tag{A.3}$$

where $\beta = \sin \pi w/2p$. The first order coefficients $C_{\pm 1}$ are calculated from:

$$C_n = \frac{1}{tS_n} - \frac{1}{|n|}, \quad n = \pm 1, \pm 2, ... \tag{A.4}$$

For TE-incidence,

$$t = j\frac{p\cos\theta}{\lambda}, \tag{A.5}$$

$$S_n = \frac{\gamma_n}{\gamma_0}, \tag{A.6}$$

$$\gamma_n = -j\sqrt{\left(\sin\theta + \frac{n\lambda}{p}\right)^2 - 1} \tag{A.7}$$

from which, it could be written that $\gamma_0 = \cos\theta$. From (A.5) and (A.6),

$$S_n t = \sqrt{\left(\frac{p\sin\theta}{\lambda} \pm n\right)^2 - \frac{p^2}{\lambda^2}} \tag{A.8}$$

and from (A.4)

$$C_n^{TE} = \frac{1}{\sqrt{\left(\frac{p\sin\theta}{\lambda} + n\right)^2 - \frac{p^2}{\lambda^2}}} - \frac{1}{|n|}. \tag{A.9}$$

Therefore,

$$C_{\pm 1}^{TE} = \frac{1}{\sqrt{\left(\frac{p\sin\theta}{\lambda} \pm 1\right)^2 - \frac{p^2}{\lambda^2}}} - 1\cdot \quad (A.10)$$

On the other hand, for TM incidence

$$t = j\frac{p\sec\phi}{\lambda}\ , \quad (A.11)$$

$$S_n = \gamma_n \gamma_0 \quad (A.12)$$

where the propagation constant γ_n is given by

$$\gamma_n = -j\sqrt{\left(\sin^2\phi + \frac{n^2\lambda^2}{p^2}\right) - 1} \quad (A.13)$$

from which, $\gamma_0 = \cos\phi$ is obtained. From (A.5) and (A.6),

$$S_n t = \sqrt{\left(\frac{p\sin\phi}{\lambda}\right)^2 + n^2 - \frac{p^2}{\lambda^2}} \quad (A.14)$$

and from (A.4),

$$C_n^{TM} = \frac{1}{\sqrt{\left(\frac{p\sin\phi}{\lambda}\right)^2 + n^2 - \frac{p^2}{\lambda^2}}} - \frac{1}{|n|} \quad (A.15)$$

and

$$C_{\pm 1}^{TM} = \frac{1}{\sqrt{1 - \left(\frac{p\cos\phi}{\lambda}\right)^2}} - 1\cdot \quad (A.16)$$

RADIOENGINEERING REVIEWERS

June 2009, Volume 18, Number 2

- ALIMENTI, F. University of Perugia, Italy
- ARCE-DIEGO, J. L. University of Cantabria, Spain
- BALDO, N. Centre Tecnologic de Telecomunica-cions de Catalunya, Spain
- BIOLEK, D., University of Defense, Brno, Czechia
- BOZZI, M., University of Pavia, Italy
- COLOMBO, A., Politecnico di Milano, Italy
- ČERNÝ, P., Czech Technical University in Prague, Czechia
- DJIGAN, V., R&D Center of Microelectronics, Russia
- DOBEŠ, J., Czech Technical University in Prague, Czechia
- DOBOŠ, L., Technical Univ. of Košice, Slovakia
- DOSTÁL, T., Brno Univ. of Technology, Czechia
- FABRE, A., Université Bordeaux, France
- GAJDOŠÍK, L., VŠB - Technical University of Ostrava, Czechia
- GRGIĆ, M., University of Zagreb, Croatia
- HÁZE, J., Brno Univ. of Technology, Czechia
- HOFFMAN, K., Czech Technical University in Prague, Czechia
- HORSKÝ, P., AMIS Czech, Ltd., Brno, Czechia
- HOSPODKA, J., Czech Technical University in Prague, Czechia
- HUDEC, P., Czech Technical University in Prague, Czechia
- HUDLIČKA, M., Czech Metrology Institute, Prague
- KASAL, M., Brno Univ. of Technology, Czechia
- KESKIN, A. U., Yeditepe Univ., Istanbul, Turkey
- KOLÁŘ, R., Brno University of Technology, Czechia
- KOLKA, Z., Brno University of Technology, Czechia
- KONOVALTSEV, A., German Aerospace Centre, Wessling-Oberpfaffenhofen, Germany
- KOS, T., University of Zagreb, Croatia
- KOVÁCS, P., Brno University of Technology, Czechia
- KRATOCHVÍL, T., Brno University of Technology, Czechia
- KULLA, P., Slovak University of Technology, Bratislava, Slovakia
- LUKEŠ, Z., Brno Univ. of Technology, Czechia
- MACI, S., University of Siena, Italy
- MATTES, M., Ecole Polytechnique Fédérale de Lausanne, Switzerland
- MARTÍN, F., Universitat Autònoma de Barcelona, Spain